Two models based on local microscopic relaxations to explain long-term basic creep of concrete

Matthieu Vandamme

PROCEEDINGS A

rspa.royalsocietypublishing.org

Research

Article submitted to journal

Subject Areas:
civil engineering, materials science

Keywords:
cement-based materials, viscosity, activation energies, soft matter

Author for correspondence:
Matthieu Vandamme
e-mail: matthieu.vandamme@enpc.fr

Two models based on local microscopic relaxations to explain long-term basic creep of concrete

Matthieu Vandamme[1]

[1]Laboratoire Navier, UMR 8205, CNRS, École des Ponts ParisTech, IFSTTAR, Université Paris-Est, Champs-sur-Marne, France

In this manuscript, we propose an exhaustion model and an adapted work-hardening model to explain the long-term basic creep of concrete. In both models, the macroscopic creep strain originates from local microscopic relaxations. The two models differ in how the activation energies of those relaxations are distributed and evolve during the creep process. With those models, at least up to a few dozen MPa, the applied stress must not modify the rate at which those relaxations occur, but only enables the manifestation of each local microscopic relaxation into an infinitesimal increment of basic creep strain. The two models capture equally well quite several phenomenological features of the basic creep of concrete. They also make it possible to explain why the indentation technique enables the quantitative characterization of the long-term kinetics of logarithmic creep of cement-based materials orders of magnitude faster than by macroscopic testing. The models hint at a physical origin for the relaxations that is related to disjoining pressures.

THE ROYAL SOCIETY PUBLISHING

1. Introduction

Since the work of Hatt in 1907 [1] and the saving of the Veurdre bridge by Freyssinet in 1912 [2], concrete is known to creep, i.e., to deform over time when subjected to a constant load. Creep of concrete impacts the durability of civil engineering infrastructures: creep can for instance lead to excessive deflections of bridges [3] or to a decrease of prestress in the confinement building of nuclear power plants [4], hence requiring monitoring, maintenance, or even sometimes replacement of the infrastructure.

Most agree that the viscous behavior of concrete mostly originates from its hydrates, and from its main constituent in ordinary Portland cement, namely calcium silicate hydrates (noted C-S-H). However, the physical origin of creep of concrete is still debated. In the short term, load-induced redistribution of water (i.e., consolidation) within the microstructure is considered to play a role [5]. For what concerns creep in a longer term, various theories have been proposed, among which: microsliding of the C-S-H layers over each other [6,7], additional self-drying due to micro-cracking [8], dissolution and then re-precipitation of the hydrates [9,10], hopping over energy barriers modified by the applied load [5], free volume dynamics [11], existence of a microprestress that impacts the apparent viscosity of the material and relaxes over time as a consequence of breakage of atomic bonds and their restoration [12]. Several of the proposed physical processes could occur concomitantly.

Time-dependent deformations of concrete are sensitive to relative humidity and can be characterized on a sample that is free to exchange moisture with its surroundings or, in contrast, on a sample that is sealed for its moisture content to remain constant. Creep of a sealed sample of concrete is characterized by applying a constant mechanical load to the sample and measuring how its strains evolve over time. However, even in absence of mechanical load, a sealed sample of concrete deforms over time, as a consequence of hydration [2], capillary effects induced by self-desiccation [13,14], and/or relaxation of eigenstresses [15]. This time-dependent strain of a sealed sample in absence of any mechanical load is called autogenous shrinkage. The difference between the time-dependent strain of a sealed sample in presence of a constant mechanical load and that of a sealed sample in absence of any mechanical load (i.e., autogenous shrinkage) is called basic creep. Thus, basic creep can be interpreted as the part of the time-dependent strain that is induced by the mechanical load.

The focus of this manuscript is basic creep, which has been extensively characterized [16,17]. In terms of phenomenology, several features can be noted. 1) Up to about 30% of its compressive strength, basic creep of mature concrete depends linearly on the applied stress [16]. 2) After some time, basic creep evolves linearly with the logarithm of time. Such qualitative feature, which manifests itself on some pre-stressed concrete bridges for instance [3], is taken into account in some codes like the fib Model Code 2010 [18] and in some models like the B4 model [17,19]. 3) The viscoelastic Poisson's ratio of concrete remains roughly constant over time for concrete samples whose elastic Poisson's ratio is comprised between 0.15 and 0.20 [20]. 4) The characteristic time to reach the logarithmic kinetics of creep increases with the age at which the sample is loaded [21]. 5) Indentation makes it possible to characterize the long-term kinetics of logarithmic creep of cement-based materials orders of magnitude faster than by macroscopic testing [22].

The objective of this manuscript is to find out a model for creep of concrete that verifies the phenomenology just described. In particular, one striking qualitative feature of concrete creep is its logarithmic evolution with time in the long term. Such kinetics is also observed on soils [23] or on metallic alloys [24]. For those latter, two models have been proposed, which make it possible to retrieve a logarithmic evolution of strains with respect to time [25]: those two models are called the exhaustion model and the work-hardening model. In those two models, the macroscopic deformation is initiated at sites whose activation requires some energy (i.e., an energy barrier needs to be overcome). The two models differ in how the activation energies are distributed and evolve during the creep process. In our manuscript, we aim at finding out whether those two models can explain basic creep of concrete and its phenomenology. We interpret the local

initiations of deformation as local microscopic relaxations. The exhaustion model is used as is, but the work-hardening model is adapted.

In section 2, we introduce the models. In section 3, we check how consistent the models are with respect to the observed phenomenology. Further discussion is performed in section 4, before we conclude.

2. Models

We consider a material loaded with a macroscopic stress Σ (see Fig. 1). In the two proposed models, we consider that the material is subjected to a succession of local microscopic relaxations. If, in absence of any macroscopic stress, a local microscopic relaxation leads to an increment of macroscopic strain (which will happen if the microscopic volume to be relaxed is prestressed/eigenstressed), with respect to the terminology commonly used to describe time-dependent deformations of concrete, this increment is interpreted as autogenous shrinkage. Here, since we are interested in basic creep, the strain of interest for our problem is the one in excess of this autogenous shrinkage, i.e., the additional incremental strain occurring during the local microscopic relaxation, as a consequence of the presence of the macroscopic stress Σ (see Fig. 1).

We consider that each local microscopic relaxation requires an activation energy U. Classically, in the spirit of the transition state theory [26], the characteristic time τ_m for this local microscopic relaxation to occur should scale with the Boltzmann distribution $\exp(U/k_BT)$, where k_B is the Boltzmann constant and T is the absolute temperature:

$$\tau_m = \tau_0 e^{U/k_BT}, \tag{2.1}$$

where τ_0 is a microscopic characteristic time. This relation has been found to correctly describe a variety of nanoscale phenomena phenomenologically, e.g., cell adhesion [27] or drying creep of nanoporous solids [28]. However, this relation is no more valid when the nanoscale processes are governed by a complex energy landscape that involves a variety of energy barriers, or in cases where the transition state theory itself breaks down.

We assume that, under the action of a macroscopic stress Σ, the local relaxation will always lead to the release of the same elastic energy, on the order of $(\Sigma^2/2E)\Omega_m$, where E is the Young's modulus of the material and Ω_m is the characteristic microscopic volume relaxed at each local microscopic relaxation. Indeed, under the assumption of linear elasticity, $(\Sigma^2/2E)\Omega_m$ is the elastic energy stored in the microscopic volume Ω_m submitted to a macroscopic stress Σ. The small increment ε_{ind} of macroscopic basic creep strain caused by each local microscopic relaxation is such that the work $\Sigma\varepsilon_{ind}\Omega$ (where Ω is the volume of the material) provided by the macroscopic stress Σ in the small increment ε_{ind} of macroscopic strain is equal to twice the elastic energy released during the relaxation (since the other half of this work is stored as an increase of elastic energy in the part of the material that was not subjected to the relaxation), i.e., $\Sigma\varepsilon_{ind}\Omega \sim (\Sigma^2/E)\Omega_m$, so that:

$$\varepsilon_{ind} \sim (\Sigma/E)(\Omega_m/\Omega). \tag{2.2}$$

Consequently, for each local microscopic relaxation event, the increment ε_{ind} of the fraction of the macroscopic strain that contributes to basic creep is proportional to the macroscopic stress Σ applied to the material.

As we will see, the two models here proposed will yield a creep function $\varepsilon(t)/\Sigma$ that evolves logarithmically with time after a transient period, i.e., that can be approximated in the long term by:

$$\varepsilon(t)/\Sigma \approx \alpha \ln(t/\tau). \tag{2.3}$$

The parameter τ will be referred as to the characteristic time of logarithmic creep, and the parameter α as to the prefactor to logarithmic creep. This prefactor, whose dimension is that of

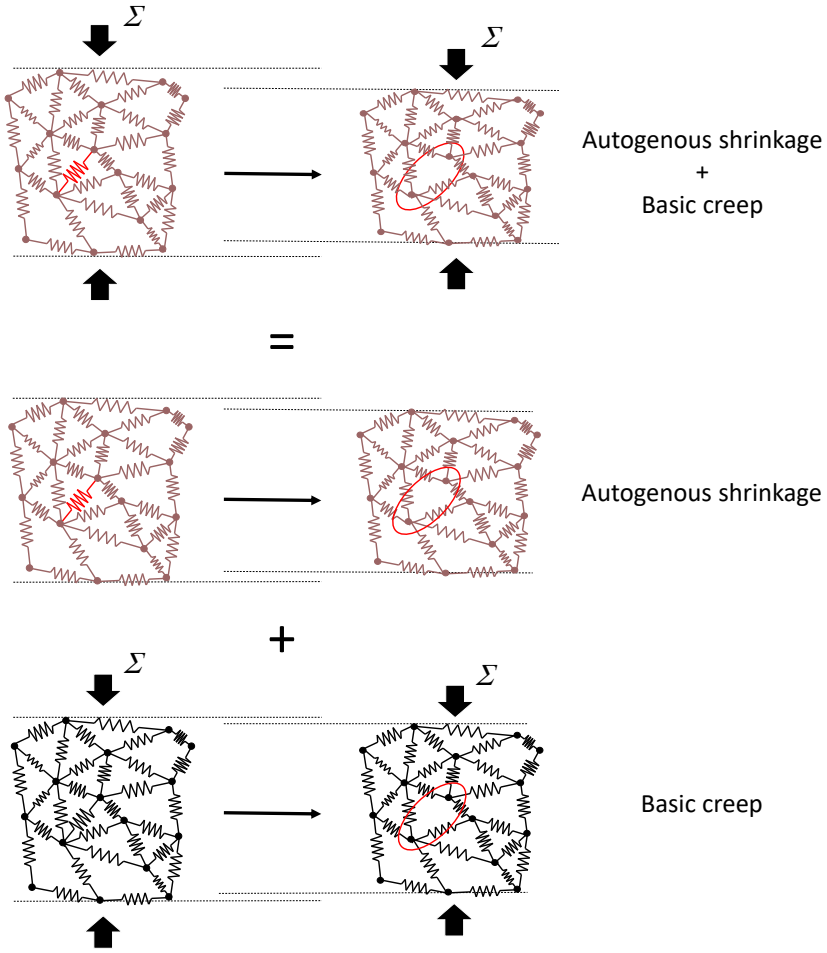

Figure 1. Strain observed during a local microscopic relaxation in presence of a macroscopic stress Σ. With respect to the classical terminology used in concrete science, this strain is the sum of autogenous shrinkage and basic creep. Autogenous shrinkage is the macroscopic strain induced by the local microscopic relaxation of a prestressed/eigenstressed microscopic element (i.e., the red spring). Basic creep is the macroscopic strain induced by the local microscopic relaxation of a microscopic element in absence of any prestress/eigenstress (i.e., the black spring) but in presence of the macroscopic stress Σ. The meaning of the colors is the following: a red spring is a microscopic element subjected to a prestress/eigenstress (i.e., a microscopic element that is stressed even when no macroscopic stress is applied); a black spring is a microscopic element submitted to no prestress/eigenstress; a brown spring is a microscopic element which may or may not be prestressed/eigenstressed.

the inverse of a stiffness, governs the long-term logarithmic kinetics of creep since, in the long term: $\dot{\varepsilon}(t)/\Sigma \approx \alpha/t$.

(a) Exhaustion model

In the exhaustion model (see Fig. 2-a), activation energies U_0 are distributed uniformly. The number of local microscopic relaxation sites with an activation energy comprised between U_0 and $U_0 + dU_0$ is noted $\bar{n}_0 dU_0$, where $\bar{n}_0$, whose dimension is the inverse of an energy, is constant. Under the action of a macroscopic stress Σ, the activation energies may be impacted. Hence, in first order, the activation energies are:

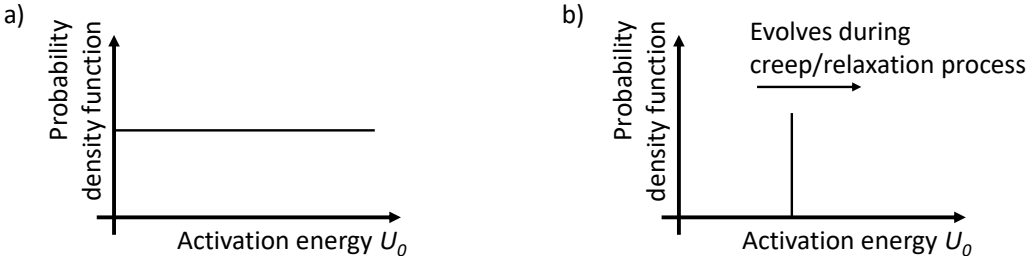

Figure 2. Probability density functions of the activation energies barriers a) in the exhaustion model and b) in the work-hardening model. The activation energy U_0 is that in absence of macroscopic stress Σ and of prestress/eigenstress σ. In the work-hardening model, the probability density function is a Dirac delta function.

$$U = U_0 - v_{exh}\Sigma, \tag{2.4}$$

where the dimension of v_{exh} is that of an energy divided by a stress, i.e., of a volume. The characteristic time for a given local relaxation to occur scales as $\tau_m = \tau_0 \exp((U_0 - v_{exh}\Sigma)/k_B T)$.

Assuming a Poisson's process for the local microscopic relaxations of sites with an activation energy (in absence of any macroscopic stress) comprised between U_0 and $U_0 + dU_0$, the fraction of those sites that will have relaxed at time t is $1 - \exp(-t/\tau_m)$. Consequently, the contribution of the relaxation of those sites to the macroscopic basic creep strain over time is: $\bar{n}_0 dU_0 (1 - e^{-t/\tau_m})\varepsilon_{ind}$. Summing over all activation energies, the macroscopic basic creep strain $\varepsilon(t)$ hence increases as:

$$\begin{aligned}\varepsilon(t) &= \int_0^{+\infty} \bar{n}_0 \varepsilon_{ind} \left(1 - e^{-t/\tau_m}\right) dU_0 \\ &= \bar{n}_0 \varepsilon_{ind} \int_0^{+\infty} \left(1 - e^{-t/\tau_m}\right) dU_0,\end{aligned} \tag{2.5}$$

which, since the microsocopic time τ_m is given by Eq. (2.1) and the activation energies by Eq. (2.4), can be solved as:

$$\begin{aligned}\varepsilon(t) &= \bar{n}_0 \varepsilon_{ind} k_B T \int_0^{(t/\tau_0)\exp(v_{exh}\Sigma/k_B T)} \frac{1 - e^{-z}}{z} dz \\ &= \Sigma \frac{\bar{n}_0 k_B T \Omega_m}{E\Omega} \left[\ln\left(\frac{t}{\tau_0}\right) + \mathrm{E1}\left(\frac{t}{\tau_0}\exp\left(\frac{v_{exh}\Sigma}{k_B T}\right)\right) + \frac{v_{exh}\Sigma}{k_B T} + \gamma\right],\end{aligned} \tag{2.6}$$

where γ is the Euler-Mascheroni constant and where E1 is an exponential integral. For large times the function E1 vanishes, so that, in the long term, the creep function $\varepsilon(t)/\Sigma$ evolves as:

$$\begin{aligned}\frac{\varepsilon(t)}{\Sigma} &\approx \frac{\bar{n}_0 k_B T \Omega_m}{E\Omega} \left[\ln\left(\frac{t}{\tau_0}\right) + \frac{v_{exh}\Sigma}{k_B T} + \gamma\right], \\ &\approx \frac{\bar{n}_0 k_B T \Omega_m}{E\Omega} \ln\left(\frac{t}{\tau_{exh}}\right), \\ \text{with } \tau_{exh} &= \tau_0 \exp\left(-\left(\gamma + \frac{v_{exh}\Sigma}{k_B T}\right)\right).\end{aligned} \tag{2.7}$$

which makes it possible to retrieve a logarithmic evolution of long-term basic creep strains.

(b) Adapted work-hardening model

In the work-hardening model (see Fig. 2-b), the activation energy U is the same at all local microscopic relaxation sites, but evolves over time. In the version of the work-hardening model proposed by Nabarro [25], the activation energies increase with strain. Here, in a dual version, we consider that there exists some microscopic prestress/eigenstress σ which impacts the energy barriers and is impacted by the local microscopic relaxations. This microscopic prestress/eigenstress is in fact present in the work-hardening model of Nabarro [25], as it intervenes in the definition of a so-called 'effective stress'. In concrete science, this microscopic prestress/eigenstress can be the micro-prestress of Bažant et al. [29] or the eigenstress of Abuhaikal et al. [15] (hence the reference to a 'prestress/eigenstress' in the caption of Fig. 1). As was the case with the exhaustion model, we also consider here that the applied macroscopic stress Σ, as well as the prestress/eigenstress σ, can impact the activation energies U, hence expressed as:

$$U = U_0 - v_{wor}^{\Sigma}\Sigma - v_{wor}^{\sigma}\sigma, \tag{2.8}$$

where U_0 is the activation energy of all local microscopic relaxation sites in absence of macroscopic stress Σ and of prestress/eigenstress σ, and where v_{wor}^{Σ} and v_{wor}^{σ} are two parameters whose dimension is that of an energy divided by a stress, i.e., a volume.

The rate at which the prestress/eigenstress σ relaxes must be proportional to the rate at which local microscopic relaxation events occurs (which is equivalent to stating that, on average, each local microscopic relaxation event relaxes the prestress/eigenstress σ by a same amount σ_{ind}), so that, in accordance with Eq. (2.1):

$$\dot{\sigma} = -\dot{\sigma_0} e^{-U/k_BT} = -\dot{\sigma_0} e^{(-U_0 + v_{wor}^{\Sigma}\Sigma + v_{wor}^{\sigma}\sigma)/k_BT}, \tag{2.9}$$

where $\dot{\sigma_0}$ is a constant parameter homogeneous to a stress divided by a time. The solution to this differential equation is:

$$\sigma(t) = \sigma_0 - \frac{k_BT}{v_{wor}^{\sigma}} \ln\left(1 + \frac{t}{\tau_{wor}}\right) \text{ with } \tau_{wor} = \frac{k_BT}{\dot{\sigma_0} v_{wor}^{\sigma}} \exp\left(\frac{U_0 - v_{wor}^{\Sigma}\Sigma - v_{wor}^{\sigma}\sigma_0}{k_BT}\right), \tag{2.10}$$

where σ_0 is the prestress/eigenstress at time $t = 0$. According to this equation, the prestress/eigenstress decreases logarithmically with respect to time. Since both the relaxation of the prestress/eigenstress $\sigma(t)$ and the increase of the basic creep strain $\varepsilon(t)$ are due to local microscopic relaxations, they must evolve in a proportional manner, from which one finds:

$$\begin{aligned} \frac{\varepsilon(t)}{\Sigma} &= \frac{k_BT\Omega_m}{v_{wor}^{\sigma} E \sigma_{ind} \Omega} \ln\left(1 + \frac{t}{\tau_{wor}}\right) \\ \text{with } \tau_{wor} &= \frac{k_BT}{\dot{\sigma_0} v_{wor}^{\sigma}} \exp\left(\frac{U_0 - v_{wor}^{\Sigma}\Sigma - v_{wor}^{\sigma}\sigma_0}{k_BT}\right), \end{aligned} \tag{2.11}$$

which also makes it possible to retrieve a logarithmic evolution of long-term basic creep strains. Indeed, in the long term:

$$\frac{\varepsilon(t)}{\Sigma} \approx \frac{k_BT\Omega_m}{v_{wor}^{\sigma} E \sigma_{ind} \Omega} \ln\left(\frac{t}{\tau_{wor}}\right). \tag{2.12}$$

3. Features of models and agreement with phenomenology

In this section, we will compare features of the models with phenomenology of basic creep of concrete. Data from macroscopic uniaxial experiments are from the database gathered by Bažant's group [30]. We only consider basic creep data on samples loaded in uniaxial compression at less

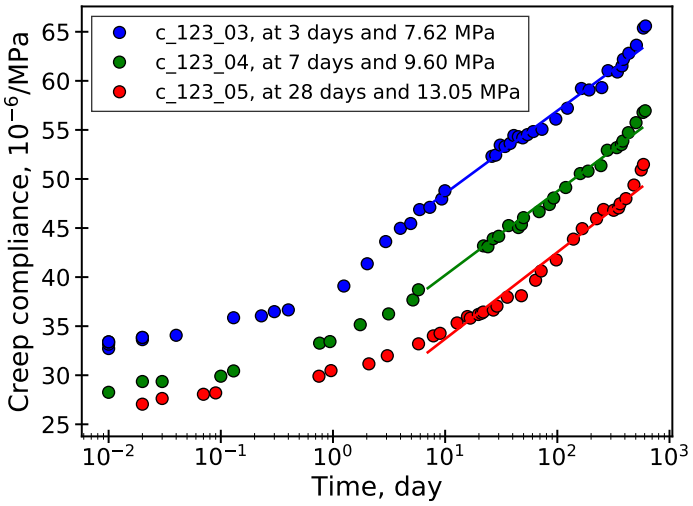

Figure 3. Examples of creep compliances measured on a given concrete at several ages and load levels by Le Roy [31]. The creep compliance is the total strain (i.e., the sum of the elastic strain and the creep strain) divided by the applied stress. The first element in the label is the file identifier in the database gathered by Bažant's group [30].

than 30% of their compressive strength, at temperatures between 15°C and 25°C, loaded at an age greater than 3 days, with no lightweight aggregates, for which if the total strain (i.e., the sum of the elastic strain and the creep strain) was given rather than the creep strain, the Young's modulus was given as well (to make it possible to calculate the creep strain). Typical measurements are displayed in Fig. 3.

(a) Linearity of creep behavior

But at the very early age (i.e., before 3 days), creep of concrete is known to be linear with respect to the applied load, up to a threshold ratio of the applied compressive stress to the compressive strength [16]. This threshold ratio is accepted to be at least equal to 30% [16], which, for a typical concrete with a compressive strength of 60 MPa, translates into a linearity of the creep behavior up to about 20 MPa of applied stress. Such linearity is for instance visible on Fig. 4, which shows that the derivative of the creep function in the long term is independent of the applied stress Σ.

An observation of Eqs. (2.7) and (2.11) shows that, for the linearity of the creep function $\varepsilon(t)/\Sigma$ to be ensured, for each model its characteristic time (i.e., τ_{exh} for the exhaustion model, and τ_{wor} for the adapted work-hardening model) must be independent of the applied macroscopic stress. For the exhaustion model, Eq. (2.7) implies that the applied macroscopic stress Σ must verify $v_{exh}\Sigma \ll k_BT$, i.e., that the applied macroscopic stress must modify the distributed activation energies by much less than k_BT. The fact that this constraint must be satisfied for a macroscopic stress of at least 20 MPa implies that the volume v_{exh} should verify $v_{exh} \ll 0.2$ nm^3. In contrast, for the adapted work-hardening model, Eq. (2.11) implies that the applied macroscopic stress Σ must verify $v^{\Sigma}_{wor}\Sigma \ll U_0 - v^{\sigma}_{wor}\sigma_0$, i.e., that the applied macroscopic stress must not modify significantly the activation energies that prevail in the material in absence of macroscopic stress (but the magnitude of those activation energies is not known).

With both models, the linearity of the basic creep strain with respect to the applied stress can be retrieved, as soon as the applied stress is sufficiently small (even though what 'sufficiently small' means differs for the two models), and, to be in accordance with experimental observations, an applied stress of 20 MPa must be sufficiently small. In turn, this constraint implies that, at least up to 20 MPa, the applied stress has no effect on the activation energies, and hence no effect on

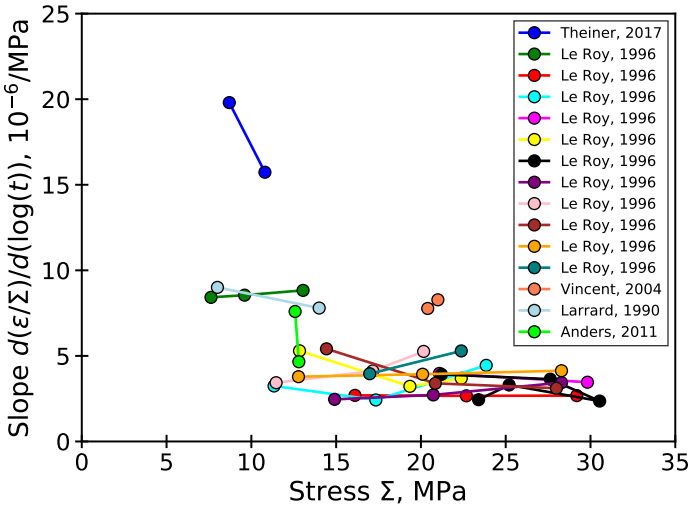

Figure 4. Slope $d(\varepsilon/\Sigma)/d(\log t)$ of the long-term creep displayed in a logarithmic scale versus the applied macroscopic stress Σ. Each curve corresponds to creep experiments performed on 1 mix design. Among the tests selected based on the criteria described at the beginning of section 3, we only considered tests for which the long-term data spanned at least one decade and for which creep experiments were performed at several loads on the same mix design. Long term was considered to start at 7 days or at three times a characteristic time introduced in the fib Model Code 2010 [18] (i.e., $3/(0.035 + 30\tau_{ref}/\tau_L)^2$, where τ_L is the age at loading and $\tau_{ref} = 1$ day), whichever was the larger. Eventually, data are from [32], [31], [33], [34], and [35].

the probability for local microscopic sites to relax. Said otherwise, local relaxations must occur in absence of macroscopic stress as often as when a macroscopic stress is applied (at least up to 20 MPa). If a macroscopic stress is applied, when those local relaxations occur, the relaxation translates into an additional increment of strain, which we interpret macroscopically as basic creep. But the applied macroscopic stress is not the reason for the local relaxation event (at least up to 20 MPa of applied macroscopic stress).

(b) Viscoelastic Poisson's ratio

Based on an analysis of the data available in the literature, Aili et al. [20] showed that the viscoelastic Poisson's ratio of concrete remains close to its elastic Poisson's ratio, when the elastic Poisson's ratio is comprised between 0.15 and 0.2, which is a typical range of values for cement-based materials. When the elastic Poisson's ratio is greater than 0.2, the viscoelastic Poisson's ratio decreases, so that its final value is comprised between 0.15 and 0.2 as well (see Fig. 5). Here, we show that the two proposed models predict evolutions of viscoelastic Poisson's ratio which are quite consistent with those experimental observations.

We define the viscoelastic Poisson's ratio as the opposite $-\varepsilon_l/\varepsilon_a$ of the ratio between lateral ε_l and axial ε_a strain during a uniaxial creep experiment. An alternative definition of a viscoelastic Poisson's ratio can be proposed based on a relaxation test, which would yield a viscoelastic Poisson's ratio that, strictly speaking, differs from the one defined on a creep experiment. However, Aili et al. [20] showed that, for cement-based materials, using one or the other definition yields viscoelastic Poisson's ratios that only differ in a negligible manner from each other in practice.

We hence consider our material subjected to a constant macroscopic stress Σ and aim at calculating how its viscoelastic Poisson's ratio evolves over time. We calculate the increments $d\varepsilon_a$ and $d\varepsilon_l$ of axial and lateral strains, respectively, which occur when an infinitesimal volume

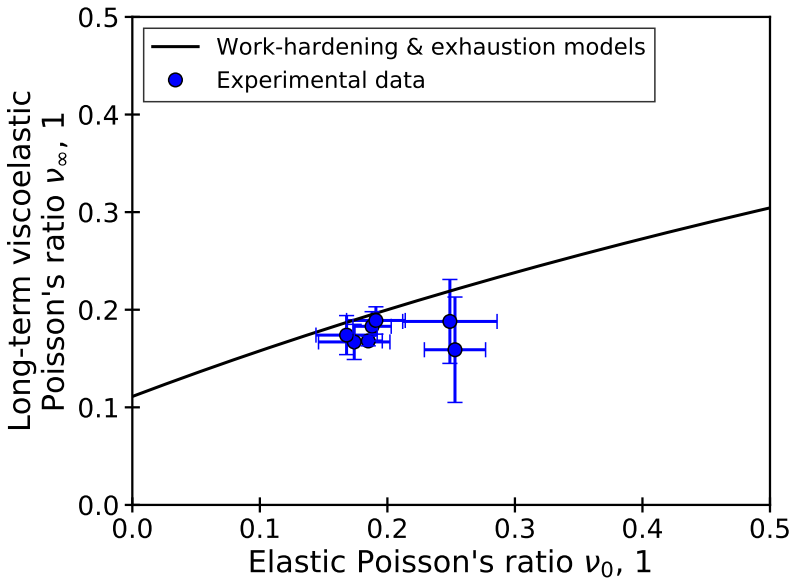

Figure 5. Long-term viscoelastic Poisson's ratio, as back-calculated from experiments and as predicted by the two models. The predictions with the work-hardening and with the exhaustion models overlap with each other. The values back-calculated from experiments come from [20].

fraction df of the material is subjected to local relaxation events. Again, as already explained in section 2, the local relaxation event itself can induce a strain (if the relaxed volume was prestressed/eigenstressed), which would be interpreted as autogenous shrinkage. But here we are interested in basic creep, i.e., in the strain that occurs during this local relaxation event in addition to autogenous shrinkage, i.e., as a consequence of the fact that the sample is under macrsocopic stress. Those infinitesimal increments $d\varepsilon_a$ and $d\varepsilon_l$ of basic creep strains occurring when an infinitesimal volume fraction df of the material is subjected to local relaxation events are the increments of strain one would observe if the relaxations would occur when the material would initially not be prestressed/eigenstressed (see Fig. 1-bottom).

We consider that the elastic properties of our material are: bulk modulus K_0 and shear modulus G_0, or, equivalently, Young's modulus $E_0 = 9K_0G_0/(3K_0 + G_0)$ and elastic Poisson's ratio $\nu_0 = (3K_0 - 2G_0)/(2(3K_0 + G_0))$. Calculating the incremental strains $d\varepsilon_a$ and $d\varepsilon_l$ is therefore equivalent to calculating the strains one expects when a volume fraction df of this material of reference is replaced by pores. The strains in this latter case can be obtained if one knows the macroscopic stiffness of the material in presence of a volume fraction df of pores. Such stiffness can be calculated with the dilute scheme model derived by Eshelby [36]. According to this model, the bulk modulus K_E and shear modulus G_E of a material whose bulk modulus of the matrix is K_0, whose shear modulus of the matrix is G_0, and that contains pores that occupy a small volume fraction f, are [37, chap. 4, sec. 3.2]:

$$K_E = K_0\left(1 - \frac{f}{1-\alpha_0}\right) \text{ and } G_E = G_0\left(1 - \frac{f}{1-\beta_0}\right), \tag{3.1}$$

where $\alpha_0 = 3K_0/(3K_0 + 4G_0)$ and $\beta_0 = 6(K_0 + 2G_0)/(5(3K_0 + 4G_0))$. Since $E_E = 9K_EG_E/(3K_E + G_E)$ and $\nu_E = (3K_E - 2G_E)/(2(3K_E + G_E))$ and since $\varepsilon_a = \Sigma/E_E$ and $\varepsilon_l = -\Sigma\nu_E/E_E$, the increments $d\varepsilon_a$ and $d\varepsilon_l$ of axial strain and radial strain, respectively, observed when a volume fraction df of the material is relaxed, can be calculated through:

$$d\varepsilon_a = \Sigma \xi_a df, \text{ where } \xi_a = \frac{1}{\Sigma}\frac{d\varepsilon_a}{df}\bigg|_{f=0} = \frac{3(5\nu_0^2 + 4\nu_0 - 9)}{2E_0(5\nu_0 - 7)}$$
$$d\varepsilon_l = \Sigma \xi_l df, \text{ where } \xi_l = \frac{1}{\Sigma}\frac{d\varepsilon_l}{df}\bigg|_{f=0} = \frac{-15\nu_0^2 + 12\nu_0 + 3}{2E_0(5\nu_0 - 7)}. \tag{3.2}$$

Under the assumption that the local stiffness does not evolve with the local relaxation event (i.e., that the local relaxation event is not a micro-cracking of the material, or does not induce any damage), radial and axial strains evolve linearly with the cumulative volume fraction $f(t)$ of material that has been subjected to local relaxation events before time t. Consequently, $\varepsilon_a(t) = \Sigma(1/E_0 + \xi_a\zeta(t))$ and $\varepsilon_l(t) = \Sigma(-(\nu_0/E_0) + \xi_l\zeta(t))$, where the function $\zeta(t)$ can be identified, with the help of Eqs. (2.6) and (2.11), with $\zeta(t) = (k_BT\Omega_m/(v^\sigma_{wor}E\sigma_{ind}\Omega\xi_a))\ln(1 + t/\tau_{wor})$ for the adapted work-hardening model and with $\zeta(t) = (\bar{n}_0 k_BT\Omega_m/(E\Omega\xi_a))[\ln(t/\tau_0) + \mathrm{E1}(t/\tau_0) + \gamma]$ for the exhaustion model, and is therefore a diverging function for both models. Finally, the viscoelastic Poisson's ratio $\nu(t)$ is found to evolve as:

$$\nu(t) = -\frac{\varepsilon_l(t)}{\varepsilon_a(t)} = \frac{\dfrac{\nu_0}{E_0} - \xi_l\zeta(t)}{\dfrac{1}{E_0} + \xi_a\zeta(t)}, \tag{3.3}$$

toward its asymptotic value ν_∞:

$$\nu_\infty = -\frac{\xi_l}{\xi_a} = \frac{5\nu_0 + 1}{5\nu_0 + 9}. \tag{3.4}$$

The asymptotic value predicted by the model is displayed in Fig. 5, together with the experimental asymptotic values given in Aili et al. [20]. With the two models, if the elastic Poisson's ratio of the material is equal to 0.2, its viscoelastic Poisson's ratio remains constant over time, which is one of the conclusions of Aili et al. [20] based on their analysis of experimental observations. With the model again, if the elastic Poisson's ratio differs from 0.2, the asymptotic value of the viscoelastic Poisson's ratio in the long term is strictly in the range between 0.2 and the elastic Poisson's ratio. As one observes in Fig. 5, the predictions of asymptotic long-term viscoelastic Poisson's ratios obtained with the model are in quite good agreement with the experimental observations. The discrepancy could be due to the heterogeneity of concrete, since the derivation performed in this section is for a homogeneous material. Discrepancy could also be due to the difficulty in measuring long-term evolutions of viscoelastic Poisson's ratios with accuracy.

(c) Measurement of creep properties by indentation

Indentation is an experimental technique to measure the mechanical properties of small volumes of materials, and in particular their creep properties [38]. Both nanoindentation [11] and microindentation [22] make it possible to characterize the long-term kinetics of logarithmic creep of cement-based materials, and provide results that are quantitatively consistent with the long-term kinetics of logarithmic creep characterized by macroscopic testing. Such consistency is surprising, because indentation experiments only last for a few minutes, while the characteristic time of logarithmic creep characterized by macroscopic testing is much longer, rather on the order of the day (see Fig. 8 or Fig. 6). The reason why indentation is able to probe this long-term kinetics is that, with indentation testing, the characteristic time of logarithmic creep is rather on the order of 1 s (see Fig. 6). However, why this characteristic time is much smaller by indentation testing than by macroscopic testing remained unclear.

Here, we aim at finding out whether the two proposed models can explain those observations. The reason that we will put forward is that stresses involved during indentation

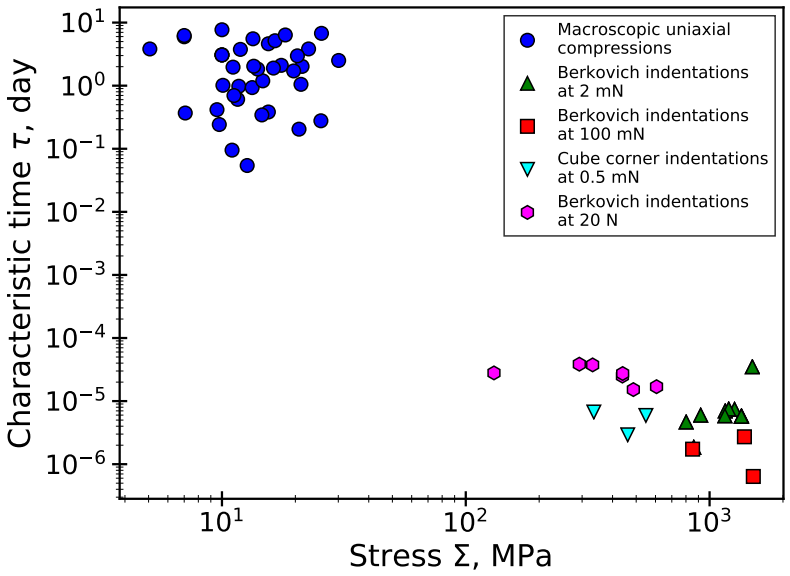

Figure 6. Impact of the applied macroscopic stress Σ on the characteristic time τ of logarithmic creep. The macroscopic uniaxial compressions are those respecting the criteria enumerated in section 3; data are from [39], [32], [40], [41], [42], [43], [31], [44], [45], [46], [33], [47], [48], [49], [34], and [35]; each data point corresponds to an average performed on all experiments on 1 mix design, independent of the load level or of the age at loading. Berkovich indentations at 2 mN and 100 mN and cube corner indentations at 0.5 mN are from [50], and Berkovich indentations at 20 N are from [22]; each data point corresponds to an average performed on all indentations performed on the hydrates of 1 mix design; the applied macroscopic stress is equal to the average of the measured indentation hardnesses.

creep experiments are much larger than stresses involved during macroscopic uniaxial creep experiments. Indeed, because of the sharpness of the Berkovich or the Cube-Corner indenter probe, stresses obtained by microindentations on cement paste or by nanoindentations on calcium silicate hydrate phases are on the order of a few hundred MPa to about 1 GPa (see Fig. 6), i.e., much higher than the stresses that are applied to macroscopic concrete samples in regular macroscopic testing.

Why large stresses could make it possible to reach the logarithmic kinetics of creep much faster than by regular macroscopic testing is readily visible from Eqs. (2.7) and (2.11): if the applied macroscopic stress is sufficiently high, it will shift the characteristic time to much lower values. For the exhaustion model, the stresses must be sufficiently high to shift the activation energies by an amount on the order of $v_{exh}\Sigma \sim k_B T$. For the adapted work-hardening model, the stresses must be sufficiently high to significantly modify the initial activation energies $U_0 - v^{\sigma}_{wor}\sigma_0$.

The other surprising feature of indentation is that its characterization of the logarithmic kinetics of creep (i.e., of the prefactor α in Eq. 2.3) is quantitatively consistent with macroscopic experiments. Here again, with the two models here proposed, the reason why it is so is clear: the prefactor in front of the logarithmic term in Eqs. (2.7) and (2.11), which governs the long-term creep rate, does not depend on the applied macroscopic stress Σ, even when this stress is arbitrarily large.

This observation makes it possible to estimate the characteristic macroscopic stress Σ_{char} below which the applied macroscopic stress Σ does not impact the probability of local microscopic relaxations, and above which it does. Indeed, the linearity of the basic creep behavior observed for stresses smaller than a few dozen MPa (see section (a)) implies that Σ_{char} is larger than a few dozen MPa. In contrast, the fact that indentation experiments make it possible to

decrease the characteristic time significantly implies that Σ_{char} must be smaller than a few hundred MPa. Consequently, the characteristic macroscopic stress Σ_{char} must be somewhere between a few dozen and a few hundred MPa. This estimate makes sense, as it is comparable to the magnitude of disjoining pressures which prevail in microporous materials (such as cement-based materials), i.e., in materials with pores smaller than 2 nm: Indeed, because of intermolecular interactions between molecules of the pore fluid and atoms of the solid skeleton, those disjoining pressures (defined as the difference between the mechanical pressure of the fluid and its thermodynamic pressure [51]) can reach characteristic magnitudes of a few hundred MPa [52], although lower [53] as well as higher values [54] are also reported (but note that the magnitude of the disjoining pressures strongly depends on the interlayer distance [55], such that the disjoining pressures in actual materials, in which only specific interlayer distances are observed, could be much lower than the maximal disjoining pressures reported in molecular simulation studies that explore a complete range of interlayer distances). This comparison of orders of magnitude hints toward local microscopic relaxations in cement-based materials which are controlled by disjoining pressure effects if the sample is not loaded mechanically or tested in regular uniaxial macroscopic experiments, but which are controlled by the applied load in indentation experiments.

In short, the models here proposed make it possible to explain why indentation decreases the characteristic time τ of logarithmic creep by several orders of magnitude (with respect to macroscopic testing) while enabling a quantitative measurement of the kinetics of this logarithmic creep (which is governed by the parameter α, see Eq. 2.3). The reason why the magnitude of the logarithmic kinetics of creep measured with indentation is quantitatively consistent with the one measured with macroscopic experiments is that the prefactors that govern this kinetics are independent of the applied stress (see Eqs. (2.7) and (2.11)). In contrast, the reason put forward for the observed decrease in characteristic time is that indentation experiments involve stresses of several hundred MPa, i.e., on the order of or even larger than disjoining pressures that prevail in microporous solids such as cement-based materials. The reasoning here performed suggests that local microscopic relaxations in cement-based materials are governed by disjoining pressure effects, except at the highest levels of stresses involved in indentation experiments.

4. Further discussion

(a) Magnitude of long-term kinetics of logarithmic creep

The prefactors in Eqs. (2.7) and (2.11), which govern the rate of the long-term logarithmic kinetics of creep, are complex, in the sense that they involve several parameters of unknown magnitude. However, some information can still be inferred from this rate, based on a more macroscopic approach. The logarithmic feature implies that, in the long term, over each decade, the same number n_{dec} of relaxation events occur, which thus relax a same volume $n_{dec}\Omega_m$ of material. Following the same logic as the one which led to Eq. (2.2), these relaxations induce an increase $\Delta_{dec}\varepsilon$ of basic creep strain over a decade which must satisfy $(\Delta_{dec}\varepsilon)\Sigma\Omega \sim (\Sigma^2/E)n\Omega_m$, so that:

$$\frac{n\Omega_m}{\Omega} \sim \frac{(\Delta_{dec}\varepsilon)E}{\Sigma}. \tag{4.1}$$

From Fig. 4, we find that $(\Delta_{dec}\varepsilon/\Sigma) = d(\varepsilon/\Sigma)/(d(\log t)) \approx 3 \cdot 10^{-6}$ MPa^{-1}. Considering a characteristic Young's modulus of 30 GPa for the concretes, we find out that the volume fraction $n\Omega_m/\Omega$ of concrete that relaxes over each decade is on the order of 10%.

Creep of concrete is accepted to originate mostly from creep of the calcium silicate hydrates. Since aggregates occupy typically around 60% to 80% of the volume of a concrete [56], since capillarity porosity occupies around 22% of the volume of cement paste for a water-to-cement mass ratio of 0.5 [56], and since calcium silicate hydrates occupy typically around 50% to 60% of the volume of solids in the hydrated cement paste [56], a typical volume fraction of calcium silicate hydrates in concrete is around 13%. From this estimation, in combination with the

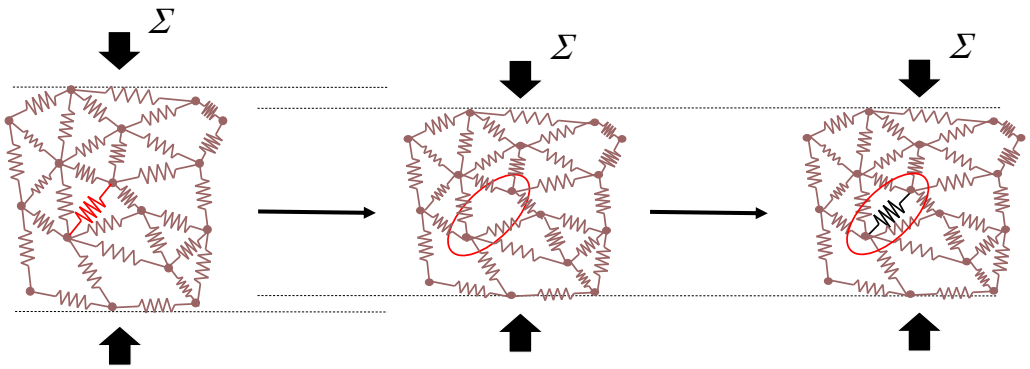

Figure 7. Envisioned process through which the local microcoscopic relaxation occurs and induces no damage. The meaning of the colors is the following: a red spring is a microscopic element subjected to a prestress/eigenstress (i.e., a microscopic element submitted to a stress, even when no macroscopic stress is applied); a black spring is a microscopic element submitted to no prestress/eigenstress; a brown spring is a microscopic element which may or may not be submitted to a prestress/eigenstress.

estimation performed in the previous paragraph, we find out that, in the long term, over each decade, most of the volume of calcium silicate hydrates is subjected to the local microscopic relaxations. Consequently, if the local microscopic relaxations were some type of micro-cracking, one would expect the material to be significantly damaged after one decade of logarithmic creep. Since, to the best of our knowledge, no significant decrease of modulus is reported for concrete during creep (again, at least up to 30% of the compressive strength), the local microscopic relaxations are not some type of micro-cracking and could rather be interpreted as some type of 'ductile' event. Indeed, concrete is known to be ductile when confinement is sufficiently high [57,58]. In our case, the ductility may be due to the confinement provided by the concrete surrounding the volume subjected to the local microscopic relaxation. Consequently, rather than what is proposed in Figure 1, a more realistic description of the local microscopic relaxation process could be the one proposed in Figure 7, in which the local microscopic relaxation induces no damage. The fact that broken bonds can be restored in geomaterials is observed experimentally, even in non-hydrating materials: indeed, TenCate et al. [59] showed that the modulus of a sample of concrete, of sandstone, or of a limestone, which decreases sharply after nonlinear acoustic straining or rapid temperature change, recovers slowly over a time (and in fact linearly with the logarithm of time).

In another manuscript [14], we confirmed that the kinetics of long-term autogenous shrinkage is consistent with the hypothesis that, in the long term, autogenous shrinkage could be due to creep of the solid skeleton under the action of capillary forces due to self-desiccation. Note that this result is not inconsistent with the idea, put forward in the present manuscript, of a viscous behavior of concrete that is governed by microscopic relaxations: in the long term, autogenous shrinkage can be driven by capillary forces which apply a mechanical stress to a solid skeleton whose viscous behavior is due to microscopic relaxations.

(b) Elements of comparison with other creep models

This idea that the mature material evolves even in absence of any applied load is consistent with the microprestress-solidification theory proposed by Bažant et al. [12]. In this theory, as a consequence of hydration and of restraint due to heterogeneity of the microstructure, micoprestresses prevail in the material, which, because of disjoining pressure effects, can reach several hundreds of MPa. Because of orientational disorder, these microprestresses, which at some location are orthogonal to the C-S-H layers, act parallel to the C-S-H layers at other locations.

The apparent viscosity of the C-S-H is considered to depend on those normal microprestresses. Parallel microprestresses induce sliding of the C-S-H layers over each other, which enables relaxation of the microprestresses, and hence yields an apparent viscosity of the C-S-H that evolves with time. The theory shows that viscosity increases linearly with time which, under load, yields a strain that increases linearly with the logarithm of time in the long term. In the microprestress-solidification theory, the applied mechanical stress has no effect on how fast the microprestresses relax. In this respect, the two models here proposed, based on the idea of local microscopic relaxations events not impacted by macroscopic applied stresses are consistent with the microprestress-solidification theory. The adapted work-hardening model relies on the existence and relaxation of a prestress/eigenstress σ (see section (b)), which is the microprestress in the microprestress-solidification theory of Bažant et al. [12], and is the eigenstress observed by Abuhaikal et al. [15]. To some extent, the adapted work-hardening model can be interpreted as a discrete version of the microprestress-solidification theory, and may provide additional physical basis to this theory. In particular, the idea that microscopic relaxations are impacted by the presence of a microscopic prestress/eigenstress is readily in line with the microprestress-solidification theory. In contrast to the microprestress-solidification theory, the models here proposed avoid having to postulate a relationship between an apparent viscosity of the material and the microprestress: the logarithmic feature of the long-term creep is a consequence of the uniform distribution of activation energies for the exhaustion model, and of the linear dependence of activation energies on stresses for the adapted work-hardening model.

It is interesting that the adapted work-hardening model provides satisfactory agreement with the phenomenology of concrete creep, although concrete is not work-hardening, but strain-softening: the mechanisms at the origin of the strain-softening behavior of concrete could differ from those at the origin of its creep behavior.

The models here proposed are quite different, in terms of spirit, from the rate theory proposed to explain creep of concrete [5] or of geomaterials [60], although the rate theory also relies on activation of local sites. In that theory, particles constituting the solid skeleton are fixed to their position by interactions with surrounding particles: schematically, they are located in a potential trough. Under the application of a macroscopic stress, the energy landscape is modified, which favors the probability of jump of the particle in some specific directions, which translates into creep. Consequently, in the rate theory, the application of a macroscopic stress modifies the activation energies. In contrast, as explained in section (a), with our models based on local microscopic relaxations, the application of a macroscopic stress (at least up to a few dozen MPa) does not modify the activation energies: local microscopic relaxations occur at a rate that is independent of this macroscopic stress, and the macroscopic stress only enables the manifestation of the local microscopic relaxation into an infinitesimal increment of basic creep strain.

(c) Evolution of characteristic time of logarithmic creep with age at loading

For concrete, the characteristic time of logarithmic creep (i.e., the parameter τ that intervenes in Eq. 2.3) is known to increase with the age of the material at which loading is initiated [61], as can be observed in Fig. 8. In this section, we aim at finding out whether this increase with the age of loading can be explained by the two proposed models.

With the exhaustion model, when loading is performed at time τ_L, if we consider the relaxation sites with an activation energy U, already a fraction $1-\exp(-\tau_L/\tau_m)$ has relaxed. When applying a macroscopic stress Σ that is sufficiently small (in the sense of the discussions of section (a), so that activation energies are not impacted by this stress), the contribution to strain of the relaxation of the remaining sites is:

$$\varepsilon(t') = \int_0^{+\infty} \bar{n}_0 \varepsilon_{ind} \left(\left(1 - e^{-\frac{t'+\tau_L}{\tau_m}} \right) - \left(1 - e^{-\frac{\tau_L}{\tau_m}} \right) \right) dU_0, \tag{4.2}$$

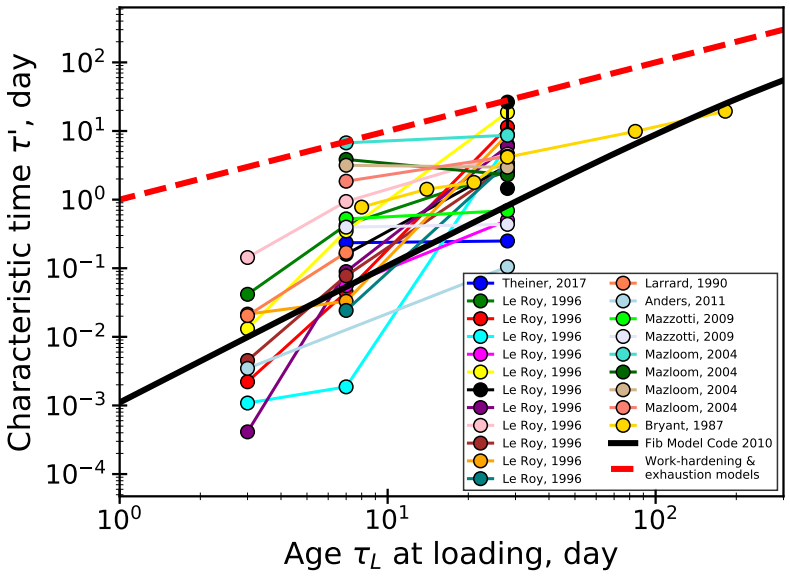

Figure 8. Impact of the age τ_L at loading on the characteristic time τ' (counted after loading) of logarithmic creep. Among the tests selected based on the criteria described at the beginning of section 3, we only considered tests for which the long-term data spanned at least one decade and for which creep experiments were performed at several ages on the same mix design. Long-term was considered to start at 7 days or at three times a characteristic time introduced in the fib Model Code 2010 [18] (i.e., $3/(0.035 + 30\tau_{ref}/\tau_L)^2$, where τ_L is the age at loading and $\tau_{ref} = 1$ day), whichever was the larger. Eventually, data are from [32], [41], [31], [46], [48], [34], and [35]. The characteristic time of logarithmic creep was calculated by fitting a line to the long-term creep data displayed on a logarithmic scale and calculating its intercept with the x-axis.

where t' is the time after loading. The solution to this equation, following the same type of derivation as in section (a), is:

$$\frac{\varepsilon(t')}{\Sigma} = \frac{\bar{n}_0 k_B T \Omega}{E \Omega_m} \left[\ln\left(\frac{t'+\tau_L}{\tau_0}\right) + \mathrm{E1}\left(\frac{t'+\tau_L}{\tau_0}\right) - \left[\ln\left(\frac{\tau_L}{\tau_0}\right) + \mathrm{E1}\left(\frac{\tau_L}{\tau_0}\right) \right] \right], \tag{4.3}$$

which in the long term is approximately equal to:

$$\begin{aligned} \frac{\varepsilon(t')}{\Sigma} &= \frac{\bar{n}_0 k_B T \Omega_m}{E \Omega} \left[\ln\left(\frac{t'+\tau_L}{\tau_0}\right) - \ln\left(\frac{\tau_L}{\tau_0}\right) - \mathrm{E1}\left(\frac{\tau_L}{\tau_0}\right) \right] \\ &= \frac{\bar{n}_0 k_B T \Omega_m}{E \Omega} \left[\ln\left(\frac{t'+\tau_L}{\tau_L}\right) - \mathrm{E1}\left(\frac{\tau_L}{\tau_0}\right) \right], \end{aligned} \tag{4.4}$$

so that the characteristic time τ'_{exh} (counted after loading) of logarithmic creep can be calculated:

$$\tau'_{exh} = \tau_L \left(\exp(\mathrm{E1}(\tau_L/\tau_0)) \right), \tag{4.5}$$

With the exhaustion model, the characteristic time of logarithmic creep increases with the age at loading, which is consistent with experimental observations. For ages τ_L at loading which are sufficiently large to satisfy $\tau_L \gg \tau_0$, the above equation becomes:

$$\tau'_{exh} \approx \tau_L. \tag{4.6}$$

One can perform the same type of calculation with the adapted work-hardening model. Akin to the logic of section (b), once the macroscopic stress Σ is applied, the basic creep strain increases

linearly with the decrease of prestress/eigenstress σ, whose expression is given in Eq. (2.11) so that:

$$\begin{aligned}\varepsilon(t') &\propto -(\sigma(t'+\tau_L)-\sigma(\tau_L))\\ \frac{\varepsilon(t')}{\Sigma} &= \frac{k_B T\Omega_m}{v^{\sigma}_{wor} C\sigma_{ind}\Omega}\left[\ln\left(1+\frac{t'+\tau_L}{\tau_{wor}}\right)-\ln\left(1+\frac{\tau_L}{\tau_{wor}}\right)\right]\\ &= \frac{k_B T\Omega_m}{v^{\sigma}_{wor} C\sigma_{ind}\Omega}\left[\ln\left(1+\frac{t'}{\tau_{wor}+\tau_L}\right)\right].\end{aligned} \tag{4.7}$$

Therefore, with the adapted work-hardening model, the characteristic time τ'_{wor} (counted after loading) of logarithmic creep verifies:

$$\tau'_{wor} = \tau_{wor} + \tau_L. \tag{4.8}$$

With the adapted work-hardening model also, the characteristic time after which creep is logarithmic increases with the age at loading, which is consistent with experimental observations.

For this feature also (i.e., how the characteristic time to reach the logarithmic kinetics of creep evolves with the age of loading), both models lead to the same phenomenology, by predicting a characteristic time that increases linearly with the age of loading. However, according to the models, this characteristic time is larger than is found experimentally, as can be observed in Fig. 8, in which we set $\tau_0 = \tau_{wor} = 1$ s. Such discrepancy is not surprising, as the main reason for aging of concrete is the evolution of hydration, which makes the mechanical properties of cement-based materials evolve over time. Also, this characteristic time to reach the logarithmic kinetics of creep may be impacted by processes specific to short-term creep (e.g., redistribution of water within the microstructure) and distinct from the local microscopic relaxations. In any case, it is interesting to observe that the two models here proposed, which disregard hydration, still predict an increase of the characteristic time with the age of loading. Consequently, in concrete, part of this observed increase could be a consequence not of hydration per se, but an intrinsic consequence of the relaxation process itself. Such idea is in line with the microprestress-solidification theory [12], in which aging of concrete is partly due to hydration (i.e., the solidification part of the theory) and partly due to a relaxation process that is independent of hydration (i.e., the microprestress part of the theory).

5. Conclusions

We proposed two models based on the idea of local microscopic relaxations to explain long-term basic creep of concrete. Those models (namely the exhaustion model and the work-hardening model), inspired from the literature on creep of metallic alloys, differ by how their activation energies are distributed and evolve during the creep process. We used the exhaustion model as is, but adapted the work-hardening model to formulate it as a function of the prestress/eigenstress prevailing in the material, rather than as a function of strain. The two models put the emphasis on stresses, activation energies, and their evolutions during the creep process, rather than on strains and evolutions of the microstructure.

Both models can be consistent with quite a large corpus of phenomenological observations on basic creep of concrete:

(i) Linearity of the basic creep behavior with the applied macroscopic stress for stresses up to about 30% of the compressive strength. To ensure this linearity, the activation energies of the local microscopic relaxation sites must not be significantly impacted by the applied macroscopic stress. Consequently, at least up to about a few dozen MPa, local microscopic relaxations must occur at a rate that is independent of the applied stress. Said otherwise, it is not the applied macroscopic stress that induces the local microscopic relaxations (i.e., it is not the modification of the energy landscape by the applied macroscopic stress that

is the reason for the creep process, as is the case in the rate theory [5]): those relaxations occur even in absence of any applied macroscopic stress but, when they occur in presence of a macroscopic stress, they translate into infinitesimal strains interpreted as basic creep. The strain induced by a local microscopic relaxation in absence of a macroscopic stress is autogenous shrinkage.

(ii) A basic creep strain that evolves linearly with the logarithm of time, after some time.

(iii) A viscoelastic Poisson's ratio that remains roughly constant over time for materials with an elastic Poisson's ratio between 0.15 and 0.2. Said otherwise, the models are also consistent with a tridimensional feature of the creep behavior. In fact, the models predict that the viscoelastic Poisson's ratio of a material with an elastic Poisson's ratio equal to 0.2 must remain constant.

(iv) Phenomenology related to indentation creep measurements, namely that indentations make it possible to reach the logarithmic kinetics of creep orders of magnitude faster than by macroscopic testing, and provide a logarithmic kinetics of creep that is quantitatively consistent with that obtained with macroscopic testing. With the models, the reason for the latter observation is that the prefactors of the logarithmic term in Eqs. (2.7) and (2.11) do not depend on the applied macroscopic stress: independent of its magnitude, the applied macroscopic stress does not modify the kinetics of logarithmic creep. In contrast, with the models, the reason for the former observation is that stresses below the indenter tip —on the order of a few hundred MPa to about 1 GPa— must be sufficiently large to significantly decrease the activation energies of the local microscopic relaxation sites. Since, as explained before, linearity of the creep behavior with respect to the applied stress observed in macroscopic testing imposes that stresses on the order of a few dozen MPa do not modify significantly these activation energies, we reach the conclusion that the characteristic magnitude of the threshold stresses that can impact activation energies must be comprised between a few dozen MPa and a few hundred MPa. Such magnitude is consistent with the magnitude of disjoining pressures which prevail in microporous systems such as cement-based materials (i.e., in porous systems with pores with a width below 2 nm), as those disjoining pressures can be on the order of a few hundred MPa. This observation hints toward activation energies of local microscopic relaxation sites which find their physical origin in the presence of disjoining pressures.

The whole phenomenology on basic creep of concrete does not allow to distinguish which of the two models (i.e., the exhaustion model or the adapted work-hardening model) is the more relevant: on the various experimental observations considered, each model is as good as the other.

With the two models here proposed, the material evolves over time, independently of the applied stress. To this respect, the proposed models are consistent with the microprestress-solidification theory of Bažant et al. [12], in which the apparent viscosity of the material evolves with time independently of the applied load. The adapted work-hardening model relies on the existence and relaxation of a prestress/eigenstress, which is the microprestress in the microprestress-solidification theory of Bažant et al. [12] and the eigenstress observed by Abuhaikal et al. [15]. To some extent, the adapted work-hardening model can be interpreted as a discrete version of the microprestress-solidification theory of Bažant et al. [12] and may provide additional physical basis to this theory.

Given that creep of soils like clays or sands is also logarithmic with respect to time in the long term, one can reasonably wonder whether the physical origin of creep for soils is the same as for cement-based materials, and whether the two proposed models (or one of the two) based on local microscopic relaxations are also relevant to explain the creep of soils. In contrast to cement-based materials, soils are materials whose chemical composition usually does not evolve over time, and whose properties are usually anisotropic: the study of creep of soils may involve challenges that differ from the study of creep of cement-based materials.

Data Accessibility. This article has no additional data.

Competing Interests. I declare no competing interest.

Funding. This work was performed while I was French-government by-fellow at Churchill College and Visitor in the Department of Engineering, at the University of Cambridge. This stay was financially supported by the Embassy of France in the United Kingdom.

Acknowledgements. I want to thank Churchill College and the Embassy of France in the United Kingdom for their support and giving me the opportunity to come and spend time as a French-government by-fellow at Churchill College and as a Visitor in the Department of Engineering at the University of Cambridge. I also want to thank Prof. Malcolm Bolton (Department of Engineering, University of Cambridge) for the interesting discussions we had around this work and around creep in general.

References

1. Hatt WK. 1907 Notes on the Effect of Time Element in Loading Reinforced Concrete Beams. In *Proc. ASTM* vol. 7 pp. 421–433.
2. Pons G, Torrenti JM. 2008 Le Retrait et Le Fluage. In *La Durabilité Des Bétons*. Presses des Ponts.
3. Bažant ZP, Hubler MH, Yu Q. 2011 Pervasiveness of Excessive Segmental Bridge Deflections: Wake-up Call for Creep. *ACI Structural Journal* **108**, 766–774.
4. Martinet E, Guinet P, Granger L, Rousselle H. 1997 Prestress Losses in NPP Containments - The EDF Experience. In *Joint WANO/OECD Workshop on Prestress Loss in NPP Containments* Poitiers, France.
5. Wittmann FH. 1982 Creep and Shrinkage Mechanisms. In *Creep and Shrinkage in Concrete Structures* pp. 129–161.
6. Tamtsia BT, Beaudoin JJ. 2000 Basic Creep of Hardened Cement Paste - A Re-Examination of the Role of Water. *Cement and Concrete Research* **30**, 1465–1475.
7. Morshedifard A, Masoumi S, Abdolhosseini Qomi MJ. 2018 Nanoscale Origins of Creep in Calcium Silicate Hydrates. *Nature Communications* **9**.
8. Rossi P, Tailhan JL, Le Maou F, Gaillet L, Martin E. 2012 Basic Creep Behavior of Concretes Investigation of the Physical Mechanisms by Using Acoustic Emission. *Cement and Concrete Research* **42**, 61–73.
9. Pachon-Rodriguez EA, Guillon E, Houvenaghel G, Colombani J. 2014 Wet Creep of Hardened Hydraulic Cements — Example of Gypsum Plaster and Implication for Hydrated Portland Cement. *Cement and Concrete Research* **63**, 67–74.
10. Pignatelli I, Kumar A, Alizadeh R, Le Pape Y, Bauchy M, Sant G. 2016 A Dissolution-Precipitation Mechanism Is at the Origin of Concrete Creep in Moist Environments. *The Journal of Chemical Physics* **145**, 054701.
11. Vandamme M, Ulm FJ. 2009 Nanogranular Origin of Concrete Creep. *Proceedings of the National Academy of Sciences of the United States of America* **106**, 10552–10557.
12. Bažant ZP, Hauggaard AB, Baweja S, Ulm FJ. 1997 Microprestress-Solidification Theory for Concrete Creep. I: Aging and Drying Effects. *Journal of Engineering Mechanics* **123**, 1188–1194.
13. Hua C, Acker P, Ehrlacher A. 1995 Analyses and Models of the Autogenous Shrinkage of Hardening Cement Paste. I. Modelling at Macroscopic Scale. *Cement and Concrete Research* **25**, 1457–1468.
14. Aili A, Vandamme M, Torrenti JM, Masson B. 2018 Is Long-Term Autogenous Shrinkage a Creep Phenomenon Induced by Capillary Effects Due to Self-Desiccation?. *Cement and Concrete Research* **108**, 186–200.
15. Abuhaikal M, Ioannidou K, Petersen T, Pellenq RJ, Ulm FJ. 2018 Le Châtelier's Conjecture: Measurement of Colloidal Eigenstresses in Chemically Reactive Materials. *Journal of the Mechanics and Physics of Solids* **112**, 334–344.
16. Neville AM, Dilger WH, Brooks JJ. 1983 *Creep of Plain and Structural Concrete*. Construction Press.
17. Bažant ZP, Jirásek M. 2018 *Creep and Hygrothermal Effects in Concrete Structures* vol. 225*Solid Mechanics and Its Applications*. Dordrecht: Springer Netherlands.
18. fib. 2013 *Fib Model Code for Concrete Structures 2010: FIB MODEL CODE 2010 O-BK*. Weinheim, Germany: Wiley-VCH Verlag GmbH & Co. KGaA.
19. RILEM Technical Committee TC-242-MDC. 2015 RILEM Draft Recommendation: TC-242-MDC Multi-Decade Creep and Shrinkage of Concrete: Material Model and Structural Analysis. *Materials and Structures* **48**, 753–770.

20. Aili A, Vandamme M, Torrenti JM, Masson B, Sanahuja J. 2016 Time Evolutions of Non-Aging Viscoelastic Poisson's Ratio of Concrete and Implications for Creep of C-S-H. *Cement and Concrete Research* **90**, 144–161.
21. Torrenti JM, Le Roy R. 2017 Analysis of Some Basic Creep Tests on Concrete and Their Implications for Modeling. pp. 1–6.
22. Zhang Q, Le Roy R, Vandamme M, Zuber B. 2014 Long-Term Creep Properties of Cementitious Materials: Comparing Microindentation Testing with Macroscopic Uniaxial Compressive Testing. *Cement and Concrete Research* **58**, 89–98.
23. Lambe TW, Whitman RW. 1969 *Soil Mechanics*. New York, NY: Wiley.
24. Nabarro FRN, DeVilliers HL. 1995 *The Physics of Creep: Creep and Creep-Resistant Alloys*. London: Taylor & Francis. OCLC: 832576348.
25. Nabarro FRN. 2001 The Time Constant of Logarithmic Creep and Relaxation. *Materials Science and Engineering A* **309-310**, 227–228.
26. Eyring H. 1935 The Activated Complex in Chemical Reactions. *The Journal of Chemical Physics* **3**, 107–115.
27. Bell GI. 1978 Models for the Specific Adhesion of Cells to Cells. *Science* **200**, 618–627.
28. Sinko R, Vandamme M, Bažant ZP, Keten S. 2016 Transient Effects of Drying Creep in Nanoporous Solids: Understanding the Effects of Nanoscale Energy Barriers. *Proceedings of the Royal Society A: Mathematical, Physical and Engineering Science* **472**, 20160490.
29. Bažant ZP, Hauggaard AB, Baweja S. 1997 Microprestress-Solidification Theory for Concrete Creep. II: Algorithm and Verification. *Journal of Engineering Mechanics-ASCE* **123**, 1195–1201.
30. Hubler MH, Wendner R, Bažant ZP. 2015 Statistical Justification of Model B4 for Drying and Autogenous Shrinkage of Concrete and Comparisons to Other Models. *Materials and Structures* **3**.
31. Le Roy R. 1996 Déformations Instantanées et Différées Des Bétons à Hautes Performances. Technical report Laboratoire Central des Ponts et Chaussées.
32. Larrard D. 1990 Creep and Shrinkage of High-Strength Field Concretes. *ACI Special Publication* **121**, 577–598.
33. Vincent EC, Townsend BD, Weyers RE, Via CE. 2004 Final Contract Report Creep of High-Strength Normal and Lightweight Concrete. Technical Report VTRC 04-CR8 Virginia Transportation Research Council Charlottesville, Virginia.
34. Anders I. 2012 *Stoffgesetz Zur Beschreibung Des Kriech- Und Relaxationsverhaltens Junger Normal- Und Hochfester Betone*. PhD thesis Karlsruher Institut für Technologie.
35. Theiner Y, Drexel M, Neuner M, Hofstetter G. 2017 Comprehensive Study of Concrete Creep, Shrinkage, and Water Content Evolution under Sealed and Drying Conditions. *Strain* p. e12223.
36. J.D. Eshelby. 1961 Elastic Inclusions and Inhomogeneities. *Progress in solid mechanics* **2**, 87–140.
37. Zaoui A. 2000 *Matériaux Hétérogènes et Composites*.
38. Vandamme M, Tweedie CCA, Constantinides G, Ulm FJ, Van Vliet KJ. 2012 Quantifying Plasticity-Independent Creep Compliance and Relaxation of Viscoelastoplastic Materials under Contact Loading. *Journal of Materials Research* **27**, 302–312.
39. Browne RD. 1967 Properties of Concrete in Reactor Vessels. In *Proceedings of the Conference on Prestressed Concrete Pressure Vessels Group C Institution of Civil Engineers* pp. 131–151 London, England. Thomas Telford Publishing.
40. Brooks JJ, Wainwright PJ. 1983 Properties of Ultra-High-Strength Concrete Containing a Superplasticizer. *Magazine of Concrete Research* **35**, 205–213.
41. Bryant AH, Vadhanavikkit C. 1987 Creep, Shrinkage-Size, and Age at Loading Effects. *Materials Journal* **84**, 117–123.
42. Russel HG, Larson SC. 1989 Thirteen Years of Deformations in Water Tower Place. *Structural Journal* **86**, 182–191.
43. Shritharan S. 1989 *Structural Effects of Creep and Shrinkage on Concrete Structures*. M. E. thesis University Auckland.
44. Huo X. 1997 *Time-Dependent Analysis and Application of High-Performance Concrete in Bridges*. PhD thesis University of Nebraska - Lincoln.
45. Navrátil J. 1998 Použití Modelu B3 pro Predikci Dotvarování a Smršťování Betonu. *Stavební obzor* pp. 110–116.
46. Mazloom M, Ramezanianpour AA, Brooks JJ. 2004 Effect of Silica Fume on Mechanical Properties of High-Strength Concrete. *Cement and Concrete Composites* **26**, 347–357.

47. Mazzotti C, Savoia M, Ceccoli C. 2005 A Comparison between Long Term Properties of Self Compacting Concretes and Normal Vibrated Concretes with Same Strength. In *Creep, Shrinkage and Durability of Concrete and Concrete Structures: CONCREEP 7* vol. 7 pp. 523–528 Nantes, France.
48. Mazzotti C, Ceccoli C. 2008 Creep and Shrinkage of Self-Compacting Concrete: Experimental Behavior and Numerical Model. In *Proceedings of the Eighth International Conference on Creep, Shrinkage and Durability Mechanics of Concrete and Concrete Structures* pp. 667–673 Ise-Shima, Japan. CRC Press.
49. Mu R, Forth JP, Beeby AW. 2008 Designing Concrete with Special Shrinkage and Creep Requirements. In *Proceedings of the Eighth International Conference on Creep, Shrinkage and Durability Mechanics of Concrete and Concrete Structures* Ise-Shima, Japan. CRC Press.
50. Vandamme M, Ulm FJ. 2013 Nanoindentation Investigation of Creep Properties of Calcium Silicate Hydrates. *Cement and Concrete Research* **52**, 38–52.
51. Coussy O. 2010 *Mechanics and Physics of Porous Solids*. Wiley.
52. Bažant ZP. 1972 Thermodynamics of Interacting Continua with Surfaces and Creep Analysis of Concrete Structures. *Nuclear Engineering and Design* **20**, 477–505.
53. Beltzung F, Wittmann FH. 2005 Role of Disjoining Pressure in Cement Based Materials. *Cement and Concrete Research* **35**, 2364–2370.
54. Karaborni S, Smit B, Heidug W, Urai J, van Oort E. 1996 The Swelling of Clays: Molecular Simulations of the Hydration of Montmorillonite. *Science* **271**, 1102–1104.
55. Pellenq RJM, Lequeux N, Van Damme H. 2008 Engineering the Bonding Scheme in C-S-H: The Iono-Covalent Framework. *Cement and Concrete Research* **38**, 159–174.
56. Mehta PK, Monteiro PJM. 2006 *Concrete: Microstructure, Properties and Materials*. McGraw-Hill 3rd edition.
57. Woolson IH. 1905 Some Remarkable Tests Indicating 'flow' of Concrete under Pressure. *Engineering News* **54**, 459–460.
58. Bazant ZP, Kim JJH, Brocca M. 1999 Finite Strain Tube-Squash Test of Concrete at High Pressures and Shear Angles up to 70 Degrees. *Materials Journal* **96**, 580–592.
59. TenCate J, Smith E, Guyer R. 2000 Universal Slow Dynamics in Granular Solids. *Physical review letters* **85**, 1020–3.
60. Kwok CY, Bolton MD. 2010 DEM Simulations of Thermally Activated Creep in Soils. *Géotechnique* **60**, 425–433.
61. Le Roy R, Le Maou F, Torrenti JM. 2017 Long Term Basic Creep Behavior of High Performance Concrete: Data and Modelling. *Materials and Structures* **50**.